PFG 2016 / 2, 085–094
Stuttgart, April 2016

Article

A Comparison of UAV- and TLS-derived Plant Height for Crop Monitoring: Using Polygon Grids for the Analysis of Crop Surface Models (CSMs)

Georg Bareth, Juliane Bendig, Nora Tilly, Dirk Hoffmeister, Helge Aasen & Andreas Bolten, Cologne

Keywords: oktocopter, laserscanning, SfM, biomass, zonal statistics

Summary: Multi-temporal crop surface models (CSMs) are a reliable method for agricultural crop monitoring. They provide 3-dimensional representations of crop canopies, preferably available as a multi-temporal dataset. From the CSMs the spatial distribution of plant height can be derived. The data for the CSMs are captured by remote sensing methods including terrestrial laser scanning (TLS) and imagery from unmanned aerial vehicles (UAVs) combined with computer vision techniques. Previous studies underlined the suitability of both methods. However, it remained an open question if both methods provide actually comparable information. We assume that the differing viewing angles of both sensors influence the resulting CSM and that the UAV-based CSMs contain crop density information due to the nadir sensor position. Therefore, we expect a lower mean plant height and higher variation in the UAV-based CSM. The correlation between plant heights from both methods was analyzed and complemented by using polygon grids for spatial analysis. The polygon grids provide descriptive statistics for each raster cell by zonal statistics to investigate the data's potential as a density measure. Through this analysis it is possible to maximize the extraction of spatial information for larger grid cells though it is not comparable to standard resampling methods. We analyzed CSMs at early, middle, and late growth stages from a barley experiment field and found a high correlation (R^2 = 0.91) in plant height derived from both methods. The UAV-derived plant height was generally lower than the TLS-derived plant height at all growth stages. However, contrary to the expectations the coefficient of variation was higher in the TLS dataset.

Zusammenfassung: *Vergleich von UAV- und TLS-abgeleiteter Pflanzenhöhe für das Monitoring von Ackerfrüchten: Die Nutzung von Polygongrids zur Analyse von Oberflächenmodellen von Getreidebeständen (CSMs).* Oberflächenmodelle von Getreidebeständen (*crop surface models*, CSMs) sind eine zuverlässige Methode für das Agrarmonitoring. Sie ermöglichen die Erstellung dreidimensionaler Modelle geschlossener Getreidebestände, vorzugsweise aus multitemporalen Datensätzen. Aus den CSMs lässt sich die räumliche Verteilung der Pflanzenhöhen ableiten. Die Erfassung der Daten erfolgt durch Fernerkundungsmethoden aus terrestrischem Laserscanning (TLS) und Aufnahmen mit unbemannten Luftfahrzeugen (*unmanned aerial vehicles*, UAVs) in Kombination mit *computer vision*-Techniken. Die Eignung beider Methoden für die nicht-destruktive Bestimmung von Pflanzenhöhe und Biomasse sind bekannt. Die noch offene Frage ist, ob beide Methoden ähnliche Informationen erfassen und inwiefern ein Vergleich der Methoden angemessen ist. Wir gehen davon aus, dass die unterschiedlichen Sensorpositionen das resultierende CSM beeinflussen. Weiterhin nehmen wir an, dass das UAV-basierte CSM aufgrund der senkrechten Sensorposition Informationen zur Bestandsdichte enthält. Folglich erwarten wir eine niedrigere mittlere Pflanzenhöhe und größere Variation in dem UAV-basierten CSM. Die Korrelation zwischen den Pflanzenhöhen beider Methoden wurde analysiert. Ergänzend wurde eine auf einem Polygongrid basierende räumliche Analyse (zonale Statistik) zur Untersuchung des Potentials der Bestandsdichteanalyse durchgeführt. Durch diese Analyse ist es möglich, den Informationsgehalt der räumlichen Daten zu maximieren. Dafür analysierten wir frühe, mittlere und späte Entwicklungsstadien in einem Gerstenexperiment und stellten eine hohe Korrelation (R^2 = 0,91) zwischen den durch beide Verfahren abgeleiteten Pflanzenhöhen fest. Die aus dem UAV-Ansatz abgeleitete Pflanzenhöhe war in allen Entwicklungsstadien 0,04 m niedriger als die aus dem TLS-Ansatz abgeleitete. Allerdings war der Variationskoeffizient, entgegen der Erwartung, im TLS-Datensatz höher (4.81% Unterschied).

www.schweizerbart.de
DOI: 10.1127/pfg/2016/0289
1432-8364/16/0289 $ 2.50

1 Introduction

Remote and proximal sensing technologies are of major importance in the context of precision agriculture (Atzberger 2013) which intends to improve nutrient, pest, and stress management to increase yield (Mulla 2013). An important crop management approach is the concept of the nitrogen nutrition index (NNI), which was introduced in the 1980s (Lemaire et al. 1984, Lemaire et al. 2008). The NNI is calculated by using the actual measured N content (N_{act}) and the critical N content (N_c) of a crop. Nc is the N content required for maximum biomass production from tillering up to flowering and is empirically determined based on the dry weight of above ground biomass (Mistele & Schmidthalter 2008a). While N_c is defined for each crop from N-experiments, the determination of N_{act} can be derived by non-destructive remote or proximal spectral measurements (Greenwood et al. 1991, 1986). The application of the NNI for in-season crop management further requires information on dry biomass. The latter can be monitored with non-destructive sensing approaches using multi- or hyperspectral sensing, laser scanning, or optical red, green, blue (RGB) imaging (Bendig et al. 2014, Ehlert et al. 2008, Gnyp et al. 2013, Hosoi & Omasa 2009, Thenkabail et al. 2000, Tilly et al. 2015).

For crop biomass monitoring, non-destructive sensor data have to be acquired according to important phenological growing stages supporting management decisions based e.g. on the before mentioned NNI. For this, the non-destructive determination of biomass is essential, because N_{act} is given in percentage of dry matter. Additionally, biomass is a key parameter for calculating the harvest index which is used for yield simulations (Kemanian et al. 2007). A typical approach to estimate biomass non-destructively is proximal or remote sensing (Mistele & Schmidthalter 2008b). Besides these approaches, it is known that plant height is a strong predictor for biomass (Catchpole & Wheeler 1992, Fricke & Wachendorf 2013). Therefore, the concept of multi-temporal Crop Surface Models (CSMs) was introduced by Hoffmeister et al. (2010) to derive plant height from terrestrial laser scanning (TLS) (Tilly et al. 2014). This concept of multi-temporal CSMs was transferred to Unmanned Aerial Vehicles (UAVs) by using RGB imaging and Structure from Motion (SfM) data analysis (Bendig et al. 2013, Cramer et al. 2013, Haala & Rothermel 2012). Plant height from UAV-derived CSMs is also used with spectral information for yield estimation (Geipel et al. 2014).

CSMs can be acquired in super-high resolution (< 0.02 m) with laser scanning techniques or from UAV imagery. And it is proven for urban environments that SfM-derived Digital Surface Models (DSMs) can produce similar data quality like TLS (Persad & Armenakis 2015, Grenzdörffer et al. 2015). A study by Ouédraogo et al. (2014) compared both methods for deriving DSMs of agricultural watersheds and found root-mean-square errors (RMSE) of 4.5 cm for TLS and 9.0 cm to 13.9 cm for the UAV-based DSM (fixed wing system) in a 12 ha watershed with 1 m × 1 m resolution. When comparing CSMs from TLS or UAV campaigns in cropping systems, a major difference is the sensor viewing geometry. This difference should be considered due to the different canopy surface roughness of varying cropping systems. While UAV approaches capture the imagery more or less in nadir view, the TLS system has an oblique acquisition position resulting in non-homogeneous point densities (Hämmerle & Höfle 2014, Ehlert et al. 2013). Consequently, the data from the two different methods should show characteristic differences in CSM-derived plant height (PH) depending on the sensor viewing geometry and the plant density (PD). In Fig. 1 the possible effect on the CSM values is shown.

The potential differences in mean plant height values shown in Fig. 1 are a result of canopy surface roughness. Variation in plant height increases with crop surface roughness. This variation should be found in data produced from nadir viewing techniques, while oblique viewing should smooth the crop surface roughness resulting in less varying plant height values. Consequently, a hypothesis of this consideration is that nadir viewing techniques for crop surfaces are a measure of crop plant height and crop plant density within one dataset. Therefore, in this study we focus on (i) the comparison of plant height data derived

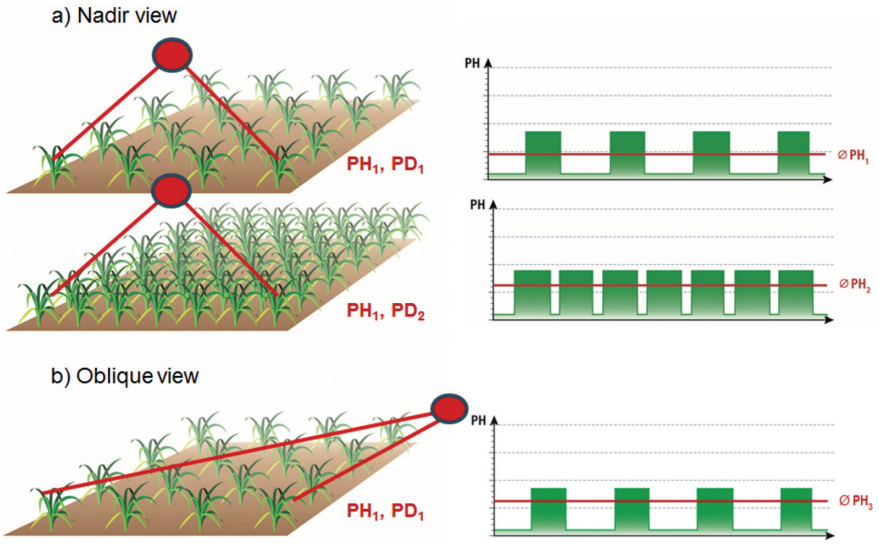

Fig. 1: The effect of different viewing geometries on the mean plant height values of crop surface models (CSMs): a) Nadir view: equal plant height (PH_1) but different plant densities (PD_1, PD_2) result in different mean plant height values ($ØPH_1 \neq ØPH_2$); b) Oblique view: equal plant height (PH_1) but different plant densities (PD_1, PD_2 (middle)) should result in similar plant height values of nadir and oblique viewing angles ($ØPH_2 \approx ØPH_3$).model projected with initial exterior orientation parameters, green = 3D building model projected with adjusted exterior orientation parameters.

from UAV imagery and TLS and on (ii) resampling methods keeping descriptive statistics of the plant height data as a density measure.

2 Material and Methods

2.1 *Study Site and Dataset*

The dataset used for the UAV and TLS comparison was partly collected within the Crop.Sense.net project activity. Crop.Sense.net was part of the German Ministry for Education and Research (BMBF) networks of excellence in agricultural and nutrition research. In this study, we used CSMs generated from the spring barley experiment site in 2013 (Tilly et al. 2015, Bendig et al. 2014). The experiment field was situated at the Campus Klein-Altendorf agricultural research station of the Agricultural Faculty, University of Bonn, Germany (50°37'51" N, 6°59'32" E, 186 m). We chose 20 preferably heterogeneous plots each 3 m × 7 m (Fig. 2) for the analysis to provide sufficient difference in plant density. Although seeding density (300 plants/m²) and row spacing (0.104 m) were identical in each plot, plant density effectively varied throughout the growing season. We analyzed data of the early (T1 = 28 May), middle (T2 = 12 June (TLS), 14 June (UAV)) and late growth stages (T3 = 10 July (TLS), 08 July (UAV)).

Fig. 2: Study site: spring barley experiment at Campus Klein-Altendorf agricultural research station; black outlines: plots, black numbers: plot numbers, background: orthophoto (28 May 2013).

2.2 *Plant Height Measurements and Crop Surface Models (CSMs)*

TLS and UAV data were captured preferably on the same day or at days close to each other. To ensure comparability, all data were georeferenced in the same coordinate system. Therefore, ground control points and scan positions were measured with a real-time kinematic global positioning system (RTK-GPS, HiPer® Pro by Topcon, Tokyo, Japan). By establishing an own reference station, a relative accuracy of 0.01 m in the horizontal and vertical was achieved.

Plant height information is derived from the CSMs representing the top canopy (Hoffmeister et al. 2010). An additional Digital Terrain Model (DTM) needs to be established prior to plant development and serves as a ground model. CSM-derived plant height is obtained by subtracting the DTM from the CSM (Bendig et al. 2013).

2.3 *UAV*

The UAV system was a MikroKopter MK-Okto (HiSystems) combined with a Panasonic Lumix GX1 digital camera (16 Megapixel, Lumix G 20 mm (F1.7 aspheric (ASPH)) fixed lens) (compare Bendig et al. 2013, 2014). The digital camera was mounted on a gimbal in nadir position. The pitch and roll movement of the UAV are compensated by the gimbal to maintain nadir imagery. Between 342 and 783 images were captured on each date at 50 m flying height, resulting in 90% forward overlap, 60% sidelap and a ground sampling distance (GSD) of 9 mm.

The imagery was processed using the SfM technique with Agisoft PhotoScan Professional software (Szeliski 2010, Sona et al. 2014). The resulting average model point density was 2,960 points/m^2. 28 ground control points served as a georeference (measured with the RTK-DGPS). The resulting CSMs were further processed in Esri ArcGIS® 10 to reduce the CSMs to the plot area of interest (AOI), to exclude plot boundaries from the analysis (0.3 m on each side), and to subtract the ground model to obtain the plant height. Prior to extraction of the area of interest, the CSMs were resampled to 10 mm raster size and smoothed using 3 × 3 pixel focal statistics (Bendig et al. 2013). It was found that smoothing had no significant effect, hence this step was neglected for future data processing. The typical height accuracy of the UAV-based CSMs lies between 15 mm – 30 mm (Grenzdörffer & Zacharias 2014, Geipel et al. 2014).

2.4 *TLS*

The TLS device was a Riegl LMS-Z420i time-of-flight scanner with a rotating polygonal mirror allowing measurement rates of up to 11,000 points/second (Riegl LMS GmbH 2015). A Nikon D200 digital camera (Nikon AF Nikkor 20 mm f/2.8D lens) and RTK-GPS receiver were mounted on the scanner additionally (Tilly et al. 2015).

The study site was scanned from its four corners with the scanner mounted on a hydraulic platform, resulting in a sensor height of 4 m above the ground. Ranging poles with highly-reflective cylinders were used to merge the scan positions during post processing. Registration, adjustment, merging, filtering of the point clouds, and the extraction of the area of interest were carried out in RiSCAN Pro. The different scan positions were registered by using the highly-reflective cylinders as tie points. Remaining alignment errors were corrected via multistation adjustment (a RiSCAN Pro functionality). Finally, the point clouds were reduced to the AOI and the maximum points were selected for the crop surface. The average point density after the filtering was 600 points/m^2 (ranging from 200–1,700 points/m^2) with the point density being very heterogeneous, due to the radial measuring principle of the static position of the TLS system. Further processing was conducted in Esri ArcGIS® 10, including the interpolation of CSMs by using the inverse distance weighting (IDW) algorithm. Afterwards, the plant heights were pixel-wise calculated by subtracting a ground model from each DSM to obtain the CSMs.

2.5 *Raster vs. Polygon Grids*

In GIS software products, zonal statistics computes descriptive statistics (minimum, maximum, range, sum, mean, standard deviation) from a value raster file for a given set of zones in raster or vector format. The descriptive statistics are calculated for each given zone by considering all raster values within a zone.

In this study, we use polygon grids for resampling and further analysis of plant height data derived from CSMs. The polygon grid represents a raster grid which stores features in vector format. Instead of resampling the super-high resolution plant height raster data to a coarser resolution, a polygon grid in a given resolution is created and serves for zonal statistics analysis in which each single polygon grid cell serves as an individual zone.

The concept is shown in Fig. 3. The coloured raster cells represent continuous plant height data in super-high spatial resolution (< 0.01 m). The black outlines represent the polygon grid in a 0.2 m resolution. Each polygon grid cell has a unique feature ID and serves as a unique zone for computing zonal statistics. The results are stored as fields in the polygon grid attribute table. In Fig. 3 the results of the zonal statistics are displayed for one polygon grid cell. The statistics are computed from the values of 1,024 raster cells.

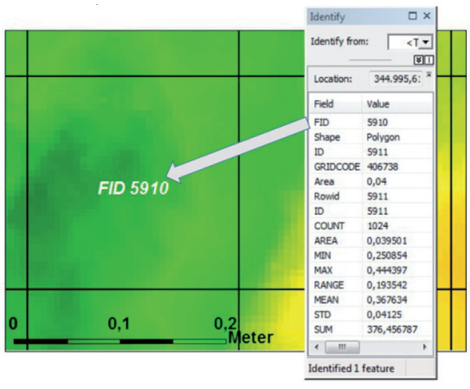

Fig. 3: Example: CSM in super-high resolution (< 0.01 m) and a corresponding polygon grid in 0.2 m resolution (black polygon outlines).

Due to the above mentioned row spacing and seeding density, a 0.3 m polygon grid was produced for this study from a resampled CSM raster by converting it into a polygon vector dataset. The resulting polygon grid served as zone data for calculating the descriptive statistics. We chose the mean plant height and the coefficient of variation (CV, i.e. the ratio of standard deviation and mean) for further analysis.

3 Results

According to the objectives of the study, the results for the comparison between UAV-derived plant heights and TLS-derived plant heights are divided into a direct comparison and the polygon grid analysis.

3.1 *UAV-CSM vs. TLS-CSM*

The comparison of TLS- and UAV-derived plant height from corresponding CSMs is presented in Fig. 4. The data represent the averaged plant height per plot of the above described barley experiment for three dates in 2013 (n = 60). As hypothesized in the introduction, the UAV-derived plant height data with nadir view have lower values compared to the TLS-derived values with the oblique view. However, the differences are much smaller than expected, but, as shown in Fig. 5, in the early growing season (T1) the differences are more characteristic than in later growth stages after canopy closure (T2). The latter is due to a smoother canopy surface. In the very late growth stage (T3) the TLS data are higher but no clear trend is observed. In general, CSM-derived plant height derived from both methods is closely related resulting in a R^2 of 0.91 overall growth stages and for T1, T2, and T3, in R^2 of 0.57, 0.72, and 0.26, respectively.

3.2 *Polygon Grids for CSM Analysis*

For this study, a 0.3 m polygon grid was produced from a resampled CSM raster by converting it into a polygon vector dataset representing continuous raster data in vector data

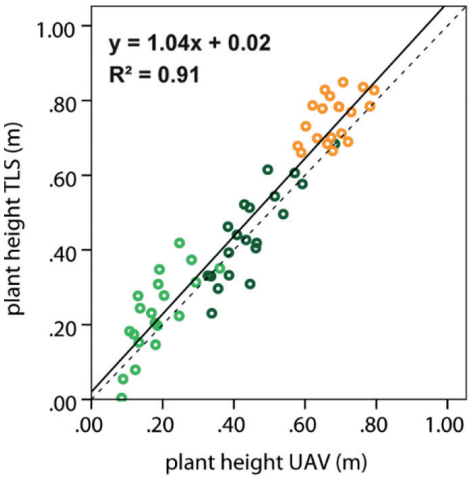

Fig. 4: Scatter plot for plant height from UAV and TLS (m) for observation dates T1 (light green), T2 (dark green), T3 (orange) (n = 60). Solid line = regression line, dashed line = 1:1 line, R^2 = coefficient of determination; p < 0.0001.

format. The resulting polygon grid serves as zone data for calculating descriptive statistics for each polygon grid cell using zonal statistics in ArcGIS®. The results for the computed mean plant height and CV are presented in Figs. 6 and 7. As already shown in Fig. 4 and hypothesized in the introduction, the mean plant heights of the UAV approach tend to be lower compared to that in the TLS approach. The difference is clearly visible in Fig. 6. Overall, the cells of the UAV polygon grid are dominated by colours representing lower plant height values than the TLS ones in all three growth stages. But surprisingly, the plant height pattern within the plots seems to be very different between the two methods in all three growth stages.

However, the computed CV shown in Fig. 7 clearly shows that the plant height values of the UAV approach vary less compared to the TLS data in all plots and in all three growth stages. Furthermore, it is again clearly visible that the two methods show different spatial patterns within the plots. This difference in the coefficient of variation was not expected and contradicts the working hypothesis that the oblique viewing angle of the TLS produces smoother surfaces with lower variance in the plant height values.

4 Discussion and Conclusion

The focus of this study was the comparison of CSM-derived plant height in agricultural crops from terrestrial laser scanning (TLS) and unmanned aerial vehicle (UAV)-based imaging by using analyses based on polygon grids. The accuracy of both the TLS-derived and the UAV-based plant height is comparable and can be used for non-destructive determination of plant height and biomass. Our previous, multi-temporal studies showed that TLS-derived plant height explained 88–95% and UAV-based plant height explained 92% of the variation in plant height compared to manual

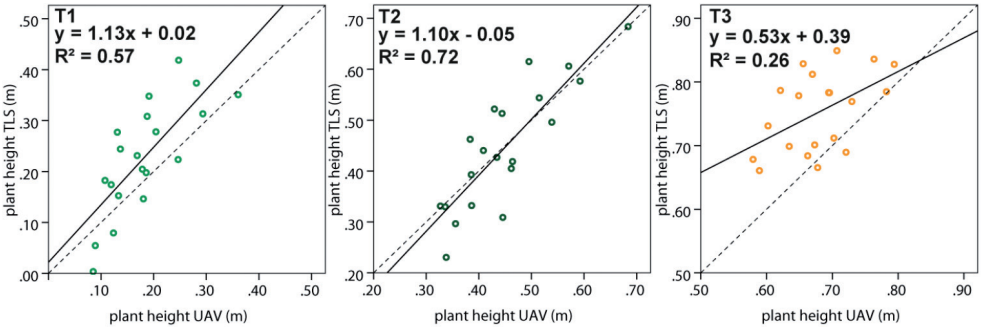

Fig. 5: Scatter plots for plant height from UAV and TLS (m) for each observation date T1, T2, and T3 (n = 20). Solid line = regression line, dashed line = 1:1 line, R^2 = coefficient of determination; p < 0.0001.

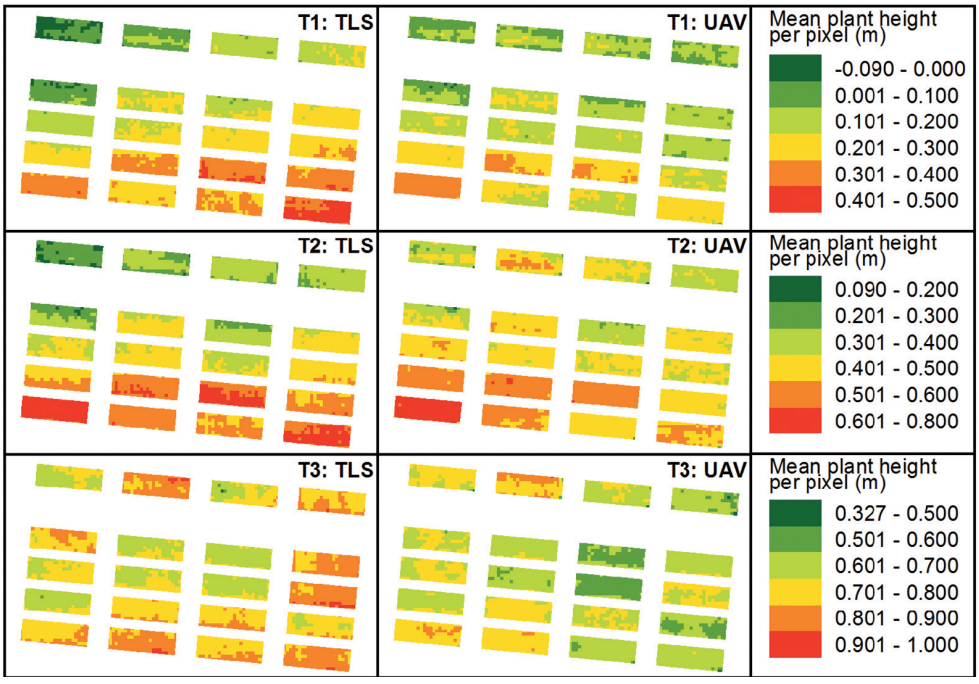

Fig. 6: Polygon grid (0.3 m pixel size) showing mean plant height per pixel for TLS and UAV.

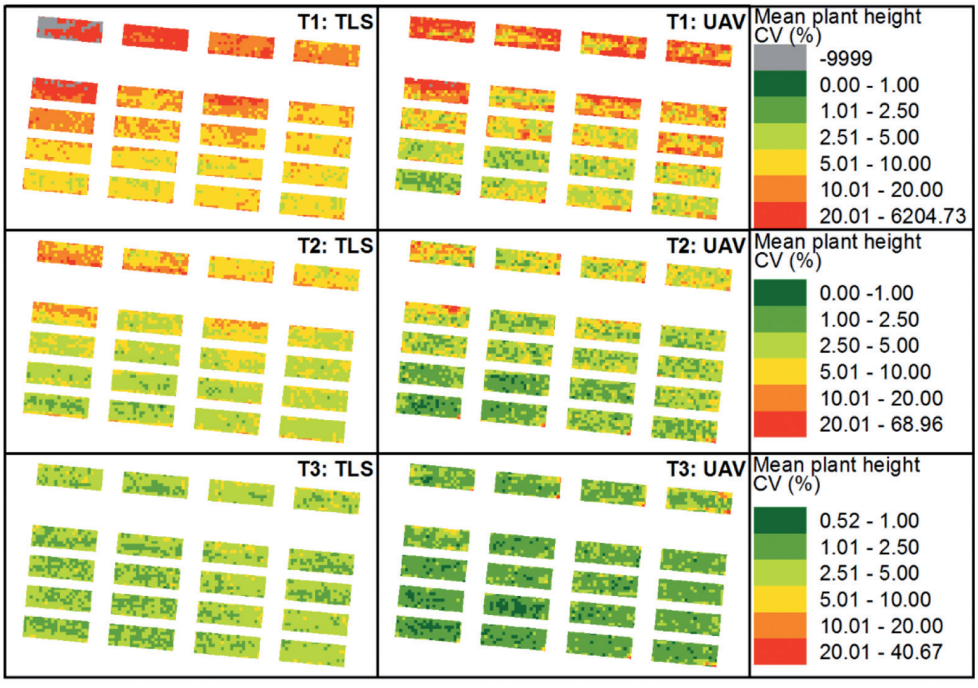

Fig. 7: Polygon grid (0.3 m pixel size) showing coefficient of variation (CV) per pixel for TLS and UAV.

measurements (Tilly et al. 2014, 2015, Bendig et al. 2013, 2014). Furthermore, the correlation is high between the TLS- and the UAV-derived plant height in this study ($R^2 = 0.91$). However, when comparing different growth stages the correlation is lower for later growth stages. A possible explanation could be that the effect of different viewing geometries increases when canopy properties change. Grenzdörffer & Zacharias (2014) indicated that wind might affect measurements in senescent grains stronger and that UAV-based plant canopies contain different numbers of soil pixels in different growth stages. The same is probably true for the TLS approach but potentially does not have a similar effect due to the differing viewing geometries. Due to calm weather conditions during the field campaigns, wind most probably did not influence our analysis.

It was hypothesized that the different viewing geometries, oblique (TLS) versus nadir (UAV), result in higher variance of the UAV-derived plant height data and in lower mean plant height values. Therefore, the nadir viewing angle provides mean plant height information which includes a plant density measure. The latter was indicated by Bareth et al. (2015) for a grassland experiment where UAV-derived plant height was evaluated against rising plate meter measurements, which represent a compressed plant density-dependent height information, resulting in an R^2 of 0.89. But in our study the introduced hypotheses could not be proofed completely. While the mean plant height values indicate the expected trend for the TLS- and UAV-based crop surface models (CSMs) with the UAV-derived values being 0.04 m lower on average, the hypothesized explanation based on the higher CSM roughness could not be proofed. We expected a higher variance in the UAV data compared to the TLS data. In fact, the coefficient of variance being 4.81% higher in the TLS data showed the contrary. The data obtained from the two different methods exhibited different spatial patterns, which were not expected either, due to the high correlation between the mean plots. A reason could be the data processing of both approaches, which includes filtering and resampling. In our study, we just compared the final processed CSM-derived plant height values. Consequently, we propose that a comparison of the original datasets, the point clouds, would be more appropriate in the future. For the latter, a key issue – and to our knowledge this was not discussed before – a new measurement protocol for the destructively measured ground truth must be developed. The traditional agronomic plant parameter measurements do not fit the accuracy of these sensing approaches. The plot-wise determination of ground truth is just not sufficient because it does not capture the spatial variability of plant height or biomass in the resolution of several cm or dm. Therefore, we propose the manual acquisition of continuous RTK-based plant-height profile measurements in the same resolution as the sensing approaches deliver. The same accounts for the biomass sampling, which must be taken from individual plant with known locations. Only with such ground truth data, the real and new potential of nadir- or oblique-derived CSMs as a plant height and plant density measure can be further investigated.

Acknowledgements

Some of the data used in this study was acquired within the CROP.SENSe.net project in context of the Ziel 2-Programm NRW 2007–2013 “Regionale Wettbewerbsfähigkeit und Beschäftigung”, financially supported by the Ministry for Innovation, Science and Research (MIWF) of the state North Rhine Westphalia (NRW) and European Union Funds for regional development (EFRE) (005-1103-0018).

References

Atzberger, C., 2013: Advances in Remote Sensing of Agriculture: Context Description, Existing Operational Monitoring Systems and Major Information Needs. – Remote Sensing **5** (2): 949–981; doi: 10.3390/rs5020949.

Bareth, G., Bolten, A., Hollberg, J., Aasen, H., Burkhart, A. & Schellberg, J., 2015: Feasibility study of using non-calibrated UAV-based RGB imagery for grassland monitoring: Case study at the Rengen Long-term Grassland Experiment (RGE), Germany. – DGPF Annual Conference’ **15:** 55–62, Cologne.

Bendig, J., Bolten, A. & Bareth, G., 2013: UAV-based imaging for multi-temporal, very high resolution crop surface models to monitor crop growth variability. – PFG – Photogrammetrie, Fernerkundung, Geoinformation **6:** 551–562; doi: 10.1127/1432-8364/2013/0200.

Bendig, J., Bolten, A., Bennertz, S., Broscheit, J., Eichfuss, S. & Bareth, G., 2014: Estimating biomass of barley using Crop Surface Models (CSMs) derived from UAV-Based RGB Imaging. – Remote Sensing **6** (11): 10395–10412; doi: 10.3390/rs61110395.

Catchpole, W.R. & Wheeler, C.J., 1992: Estimating plant biomass: A review of techniques. – Australian Journal of Ecology **17:** 121–131; doi: 10.1111/j.1442-9993.1992.tb00790.x.

Cramer, M., Haala, N., Rothermel, M., Leiness, B. & Fritsch, D., 2013: UAV@LGL – Pilot Study of the Use of UAV for National Mapping in Germany. – PFG – Photogrammetrie, Fernerkundung, Geoinformation **5:** 495–509; doi: 10.1127/1432-8364/2013/0195.

Ehlert, D., Horn, H.-J. & Adamek, R., 2008: Measuring crop biomass density by laser triangulation. – Computers and Electronics in Agriculture **61:** 117–125.

Ehlert, D. & Heisig, M., 2013: Sources of angle-dependent errors in terrestrial laser scanner-based crop stand measurement. – Computers and Electronics in Agriculture **93:** 10–16.

Fricke, T. & Wachendorf, M., 2013: Combining ultrasonic sward height and spectral signatures to assess the biomass of legume-grass swards. – Computers and Electronics in Agriculture **99:** 236–247.

Geipel, J., Link, J. & Claupein, W., 2014: Combined spectral and spatial modeling of corn yield based on aerial images and crop surface models acquired with an unmanned aircraft system. – Remote Sensing **6:** 10335–10355.

Gnyp, M.L., Yu, K., Aasen, H., Yao, Y., Huang, S., Miao, Y. & Bareth, G., 2013: Analysis of Crop Reflectance for Estimating Biomass in Rice Canopies at Different Phenological Stages. – PFG – Photogrammetrie, Fernerkundung, Geoinformation **4:** 351–365; doi: 10.1127/1432-8364/2013/0182.

Greenwood, D.J., Neeteson, J.J. & Drayvott, A., 1986: Quantitative relationships for the dependence of growth rate of arable crops on their nitrogen content, dry weight and aerial environment. – Plant and Soil **91** (3): 281–301.

Greenwood, D.J., Gastal, F., Lemaire, G., Draycott, A., Millard, P. & Neeteson, J.J., 1991: Growth Rate and % N of Field Grown Crops: Theory and Experiments. – Annals of Botany **67** (2): 181–190.

Grenzdörffer, G.J., Naumann, M., Niemeyer, F. & Frank, A., 2015: Symbiosis of UAS Photogrammetry and TLS for Surveying and 3D Modelling of Cultural Heritage Monuments – A Case Study about the Cathedral of St. Nicholas in the City of Greifswald. – ISPRS – International Archives of the Photogrammetry, Remote Sensing and Spatial Information Sciences XL-1/W4: 91–96; doi: 10.5194/isprsarchives-XL-1-W4-91-2015.

Grenzdörffer, G. & Zacharias, P., 2014: Bestandshöhenermittlung landwirtschaftlicher Kulturen aus UAS-Punktwolken. – 34. Wissenschaftlich-Technische Jahrestagung der DGPF, Hamburg.

Haala, N. & Rothermel, M., 2012: Dense Multi-Stereo Matching for High Quality Digital Elevation Models. – PFG – Photogrammetrie, Fernerkundung, Geoinformation **4:** 331–343; doi: 10.1127/1432-8364/2012/0121.

Hämmerle, M. & Höfle, B., 2014: Effects of reduced terrestrial LiDAR point density on high-resolution grain crop surface models in precision agriculture. – Sensors **14** (12): 24212–24230; doi: 10.3390/s141224212.

Hoffmeister, D., Bolten, A., Curdt, C., Waldhoff, G. & Bareth, G., 2010: High-resolution Crop Surface Models (CSM) and Crop Volume Models (CVM) on field level by terrestrial laser scanning. – Guo, H. & Wang, C. (eds.): SPIE Sixth International Symposium on Digital Earth: Models, Algorithms, and Virtual Reality. – Beijing, China: 78400E–78400E6.

Hosoi, F. & Omasa, K., 2009: Estimating vertical plant area density profile and growth parameters of a wheat canopy at different growth stages using three-dimensional portable lidar imaging. – ISPRS Journal of Photogrammetry and Remote Sensing **2** (64): 151–158.

Kemanian, A.R., Stöckle, C.O., Huggins, A.R. & Viega, L.M., 2007: A simple method to estimate harvest index in grain crops. – Field Crops Research **103** (3): 208–216.

Lemaire, G., Jeuffroy, M.-H. & Gastal, F., 2008: Diagnosis tool for plant and crop N status in vegetative stage: Theory and practices for crop N management. – European Journal of Agronomy **28** (4): 614–624.

Lemaire, G., Salette, J., Sigogne, M. & Terrasson, J.-P., 1984: Relation entre dynamique de croissance et dynamique de prélèvement d'azote pour un peuplement de graminées fourragères. I. – Etude de l'effet du milieu. – Agronomy for Sustainable Development **4** (5): 423–430; doi: 10.1051/agro:19840503.

Mistele, B. & Schmidthalter, U., 2008a: Estimating the nitrogen nutrition index using spectral canopy reflectance measurements. – European Journal Agronomy **29:** 184–190.

Mistele, B. & Schmidthalter, U., 2008b: Spectral measurements of the total aerial N and biomass dry weight in maize using a quadrilateral-view optic. – Field Crops Research **106** (1): 94–103.

Mulla, D.J., 2013: Twenty five years of remote sensing in precision agriculture: key advances and remaining knowledge gaps. – Biosystems Engineering **114** (4): 358–371.

Persad, R.A. & Armenakis, C., 2015: Alignment of Point Cloud DSMs from TLS and UAV Platforms. – ISPRS – International Archives of the Photogrammetry, Remote Sensing and Spatial Information Sciences XL-1/W4: 369–373; doi: 10.5194/isprsarchives-XL-1-W4-369-2015.

Ouédraogo, M.M., Degré, A., Debouche, C. & Lisein, J., 2014: The evaluation of unmanned aerial system-based photogrammetry and terrestrial laser scanning to generate DEMs of agricultural watersheds. – Geomorphology **214:** 339–355.

Riegl LMS GmbH, 2015: Datasheet Riegl LMS-Z420i. – http://www.riegl.com/uploads/tx_pxpriegldownloads/10_DataSheet_Z420i_03-05-2010.pdf (1.9.2015).

Sona, G., Pinto, L., Paglirai, D., Passoni, D. & Gini, R., 2014: Experimental analysis of different software packages for orientation and digital surface modelling from UAV images. – Earth Science Informatics **7:** 97–107; doi: 10.1007/s12145-013-0142-2.

Szeliski, R., 2010: Computer Vision: Algorithms and Applications. – 824 p., Springer, London, UK.

Thenkabail, P.S., Smith, R.B. & De Pauw, E., 2000: Hyperspectral Vegetation Indices and their relationships with agricultural crop characteristics. – Remote Sensing Environment **71** (2): 158–182.

Tilly, N., Hoffmeister, D., Ciao, Q., Huang, S., Miao, Y., Lenz-Wiedemann, V. & Bareth, G., 2014: Multi-temporal Crop Surface Models: Accurate plant height measurement and biomass estimation with terrestrial laser scanning in paddy rice. – Journal of Applied Remote Sensing **8** (1): 083671-1–083671-22; doi: 10.1117/1.JRS.8.083671.

Tilly, N., Aasen, H. & Bareth, G., 2015: Fusion of plant height and vegetation indices for the estimation of barley biomass. – Remote Sensing **7** (9): 11449–11480; doi: 10.3390/rs70911449.

Addresses of the Authors:

Prof. Dr. Georg Bareth, Dr. Juliane Bendig, Nora Tilly, Dr. Dirk Hoffmeister, Helge Aasen & Dr. Andreas Bolten, Institute of Geography, GIS & RS Group, University of Cologne, Albertus-Magnus-Platz, D-50923 Köln, Tel.: +49-221-470-6551, Fax: +49-221-470-1638, e-mails:{g.bareth}{juliane.bendig}{nora.tilly}{dirk.hoffmeister}{helge.aasen}{andreas.bolten}@uni-koeln.de

Manuskript eingereicht: Oktober 2015
Angenommen: Januar 2016